Transport Properties of some Deprivatives of Tetrathiafulvalenetetracyano-p-quinodimethane (TTF-TCNQ)

Jacobsen, Claus Schelde; Mortensen, Kell; Andersen, Jan Rud; Bechgaard, K.

Published in:
Physical Review B

Link to article, DOI:
10.1103/PhysRevB.18.905

Publication date:
1978

Document Version
Publisher's PDF, also known as Version of record

Transport properties of some derivatives of tetrathiafulvalene-tetracyano-*p*-quinodimethane (TTF-TCNQ)

C. S. Jacobsen and Kell Mortensen
Physics Laboratory III, Technical University of Denmark, DK-2800 Lyngby, Denmark

J. R. Andersen
Chemistry Department, Risø National Laboratory, DK-4000 Roskilde, Denmark

K. Bechgaard
Department of General and Organic Chemistry, H. C. Ørsted Institute, DK-2100 Copenhagen, Denmark
(Received 14 March 1978)

Data on dc conductivity $\sigma(T)$ and thermoelectric power $S(T)$ for four organic conductors related to tetrathiafulvalene-tetracyano-*p*-quinodimethane (TTF-TCNQ) are presented. They all qualitatively behave as TTF-TCNQ with metal-insulator (M-I) transitions at temperatures around 50 K. Tetramethyltetraselenafulvalene-tetracyano-*p*-quinodimethane (TMTSeF-TCNQ) has $\sigma(300\ \mathrm{K}) = 1000\ \Omega^{-1}\mathrm{cm}^{-1}$, $\sigma_{max}/\sigma(300\ \mathrm{K}) = 7$, $S(300\ \mathrm{K}) = 8\mu\mathrm{V/K}$. For tetramethyltetraselenafulvalene-dimethyltetracyano-*p*-quinodimethane (TMTSeF-DMTCNQ) $\sigma(300\ \mathrm{K}) = 500\ \Omega^{-1}\mathrm{cm}^{-1}$, $\sigma_{max}/\sigma(300\ \mathrm{K}) = 10$, $S(300\ \mathrm{K}) = 11\ \mu\mathrm{V/K}$. The sulphur analogue tetramethyltetrathiafulvalene-dimethyltetracyano-*p*-quinodimethane (TMTTF-DMTCNQ) has $\sigma(300\ \mathrm{K}) = 120\ \Omega^{-1}\mathrm{cm}^{-1}$, $\sigma_{max}/\sigma(300\ \mathrm{K}) = 3$, $S(300\ \mathrm{K}) = -30\ \mu\mathrm{V/K}$, while for diethyldimethyltetraselenafulvalene-tetracyano-*p*-quinodimethane (DEDMTSeF-TCNQ) we find $\sigma(300\ \mathrm{K}) = 500\ \Omega^{-1}\mathrm{cm}^{-1}$, $\sigma_{max}/\sigma(300\ \mathrm{K}) = 9$, $S(300\ \mathrm{K}) = 18\mu\mathrm{V/K}$. $S(T)$ for the selenium-containing materials is small and metallic above the M-I transitions. $S(T)$ for TMTTF-DMTCNQ is high and negative with only slight temperature dependence above 100 K. TMTTF-DMTCNQ and TMTSeF-DMTCNQ are discussed in terms of a simple model of independent stacks. The transport on the DMTCNQ stacks is found to be diffusive while the TMTSeF stacks are in the band regime. Polarized-reflectance data are given for TMTSeF-TCNQ, TMTSeF-DMTCNQ, and TMTTF-DMTCNQ. A plasma edge in the near infrared is found in all cases. The small shifts observed are interpreted as arising from variations in effective bandwidths and degrees of charge transfer. The extrapolated zero-frequency optical conductivity is similar in all materials and greater than the measured dc conductivities, indicating different relaxation mechanisms at dc and at optical frequencies. In the M-I transition region zero crossings of $S(T)$ are generally found and at low temperatures both $\sigma(T)$ and $S(T)$ show semiconducting behavior. Exceptions are TMTSeF-DMTCNQ doped with methyl-TCNQ (MeTCNQ) and DEDMTSeF-TCNQ, where the transitions are smeared. This smearing is attributed to static disorder.

I. INTRODUCTION

An obvious extension of the efforts to elucidate the transport properties of the quasi-one-dimensional organic conductor tetrathiafulvalene-tetracyano-*p*-quinodimethane (TTF-TCNQ),[1,2] is to investigate analogous compounds. Information on the influence of minor changes in electronic structure of the constituent molecules and of changes in crystal packing on the physical properties of the solids may be obtained to this manner.

New properties have thus been observed for example in the systems hexamethylenetetrathiafulvalene-TCNQ-(HMTTF-TCNQ),[3,4] and hexamethylenetetraselenafulvalene-TCNQ (HMTSeF-TCNQ),[5] where a small change of geometry of the donor (relative to TTF) produces a different crystal structure in which the metallic regime is stablized to temperatures as low as 15 mK. This is in contrast to TTF-TCNQ, where the onset of a metal-insulator transition at temperatures lower than 60 K makes the material semiconducting.

We present results for solids derived from the prototype TTF-TCNQ, in which modifications have been made by exchange of heteroatoms in the donor and/or by attachment of small aliphatic substituents to both donor and acceptor molecules. The present work focuses on the properties of two systems, tetramethyltetraselenafulvalene-dimethyltetracyano-*p*-quinodimethane (TMTSeF-DMTCNQ) and tetramethyltetrathiafulvalene-DMTCNQ(TMTTF-DMTCNQ), but we also present data for TmTSeF-TCNQ and diethyldimethyltetraselenafulvalene-TCNQ (DEDMTSeF-TCNQ), and on TMTSeF-DMTCNQ, doped with methyl-TCNQ (MTCNQ) (see Fig. 1 for molecular structure and names of constituent molecules).

Our interest in TMTSeF-DMTCNQ originated from the observation of a single very sharp anomaly at 42 K in the electrical conductivity[6] in-

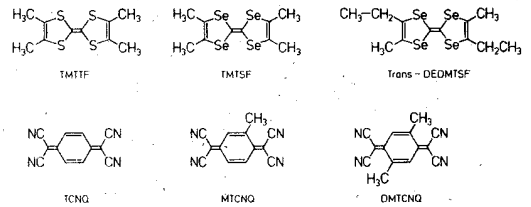

FIG. 1. Molecular design.

dicating that a first-order transition might occur. However, since structural information at low temperature is not at present available we shall not consider this particular problem. The room-temperature structure of TMTSeF-DMTCNQ is triclinic and exhibits the usual segregated stacks of these materials with interplanar spacing of 3.64 and 3.31 Å, respectively.[7] An interesting feature is the fact that the molecular overlap in the acceptor stacks is not symmetric (see Fig. 2). This allows first-order electron-libron coupling (see below).

The structure of TMTTF-DMTCNQ has not been solved in detail but indexing of powder diffraction data[8] has shown that it is iso-structural with TMTSeF-DMTCNQ, thereby making a direct comparison of the physical properties of the two systems reasonable. The structure of TMTSeF-TCNQ has also been solved in detail.[9] Again a triclinic system is found but the arrangement of stacks is rather different from the two DMTCNQ compounds, and the overlap is highly symmetric in both donor and acceptor stacks. DEDMTSeF-TCNQ yields crystal of rather poor quality and no exact diffraction data have been obtained.[10] However,

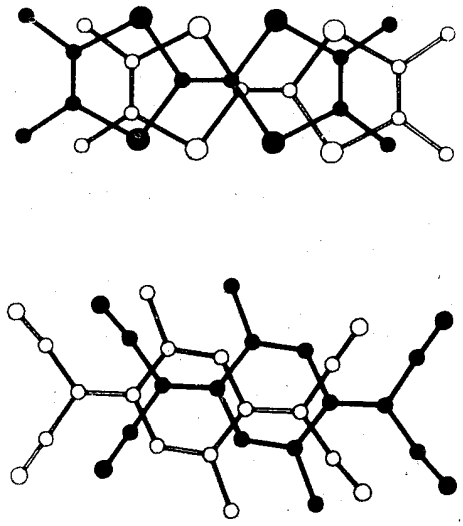

FIG. 2. Stacking patterns of TMTSeF and DMTCNQ molecules in TMTSeF-DMTCNQ (Ref. 7) viewed along the normals to the molecular planes.

this salt is of considerable interest for two reasons. (i) The bulky ethyl groups are expected to reduce intermolecular overlaps significantly and (ii) static disorder in the crystal is likely, since the DEDMTSeF molecules probably are present in both *cis* and *trans* configurations (see Fig. 1).

In the present study we have investigated transport properties by three means. Thermoelectric power and dc conductivity give information about transport regimes and carrier signs, and optical spectroscopy in the intraband region yield data on carrier concentrations and bandwidths. In the paper we attempt a tentative decomposition of the high-temperature transport properties of the DMTCNQ salts into separate donor and acceptor stack contributions. We compare dc and optical conductivities, and after commenting on the possible transport mechanisms, we finally discuss the temperature region around and below the metal-insulator transitions.

Most of the data presented here are new. We have previously reported preliminary conductivity data on TMTSeF-DMTCNQ (Ref. 6) and Bloch and coworkers[2,11] have reported the temperature-dependent dc conductivity of TMTSeF-TCNQ. Our results are in excellent agreement with theirs.

Of other than transport measurements, the study of Tomkiewicz *et al.*[12] on the magnetic properties of TMTSeF-DMTCNQ is of special interest. They find donor stack dominance in agreement with the conclusions of the present transport study.

II. EXPERIMENTAL

A. Sample preparation and characterization

TMTSeF,[13] TMTTF,[14] TCNQ,[15] MeTCNQ,[15] and DMTCNQ[6] were prepared according to procedures in the literature, and DEDMTSeF by a route analogous to that of TMTSeF. All compounds were purified by multiple recrystallization followed by one or more gradient sublimations onto Teflon. Solvents used for recrystallization and crystal growing were analytical grade and further purified by distillation and dried by passage of alumina (Woelm, Super 1), deoxygenated by purging with argon, and stored in sealed siphon bottles until used.

All the crystals of the five solids in question were prepared by slow evaporation of solvent from saturated solutions. In a typical experiment TMTSe (24 mg) was dissolved in 20 ml CH_2Cl_2, DMTCNQ (13 mg) was dissolved in 20 ml CH_3CN, and the two solutions mixed at 40 °C in a long-necked volumetric flask (50 ml). After 5 days at 40 °C (5–10 ml left-over of solvent) in the dark in inert atomosphere the crystals were harvested, washed with a little dry ether, and dried in vacuo.

The yield was 78% dark shiny needles analyzing precisely as $(TMTSeF)_1$-$(DMTCNQ)_1$ (C, H, N).

TMTTF-DMTCNQ, TMTSeF-TCNQ, and DEDMTSeF-TCNQ were grown under similar conditions from the same solvent mixture at 40 °C. Due to difference in solubility, starting concentrations were approximately 0.5, 1.0, and 2.0 mg/ml for the three salts, respectively. These complexes also gave very accurate analyses for 1:1 stochiometry.

All the crystals are black, shiny needles, but of different qualities and mechanical properties. The TMTSeF-TCNQ samples are prismatic, about 2 $\times 0.2 \times 0.05$ mm, with well-shaped optical faces. They are quite brittle, but are easily cut to desired dimensions. The other three materials tend to grow in assemblies and are severely damaged when cut. They do not break, but are deformed just like a bunch of fibers. To avoid this the crystals may be shortened by etching. DEDMTSeF-TCNQ was only available as very thin crystals with cross sections of about 20×30 μm. This fact made it impossible to obtain optical data of acceptable quality. The available DMTCNQ salt crystals are about 0.1×0.1 mm in cross section. The TMTSeF type is clearly of higher quality than the TMTTF type, but with some care acceptable samples of both materials were selected.

B. Measuring techniques

The measuring techniques used to determine conductivity, thermoelectric power, and optical properties are described in the following. The dc conductivity was measured using standard four-probe techniques. The sample mounting was similar to that described by Coleman,[16] using 13- or 25-μm diam 99.99% annealed Au wire and silverpaste for contacting. In some cases Al contacts were evaporated onto the crystals. Such contacts were found to be more stable than silverpaste contacts on very thin crystals, where the contact areas necessarily are small. Contact resistances were found to approximately scale with contact areas and were for all accepted mountings in the range from 5 to 100 Ω. Normal measuring currents did not exceed 50 μA in the conducting regime, while much smaller current levels were used in the semiconducting low-temperature regime. In all cases ohmic behavior was found. Measurements were performed at 14.5 Hz with frequent checks at dc.

For some of the materials the crystals were of adequate quality to measure anisotropies. This was done using the Montgomery method,[17] where contacts are made to the four corners of the crystal.

Details in the resistivity around the transition anomalies were studied in two ways. First, by a continuous $R(T)$ measurement, where an XY recorder plots R vs T, while the sample holder is drifting very slowly through the interesting temperature region. After this the curve can be differentiated manually to give for example $d\ln R/d(1/T)$. The second, more sensitive technique is based on a modulation method. A small quartz block in contact with a temperature-controlled heat reservior is equipped with a thin-film Nichrome heater. Four 25-μm diam gold wires are thermally anchored to the quartz block and provide electrical as well as thermal contact to the sample. The power to the heater is square wave modulated and a dc current is sent through the sample. Then the dc component of the voltage drop is proportional to the resistance R, and the ac component is proportional to dR/dT. In the actual experiment the amplitude of the temperature modulation is kept below 0.02 K and the frequency is a few hertz. A typical time constant for the sample is 50 msec in the temperature range 30–60 K.

The technique used for measurements of thermopower is similar to that described by Chaikin and Kwak.[18] A slow ac technique is employed making a maximum temperature drop across the sample of less than 0.5 K. The thermopower S is measured against that of pure gold, and reference thermocouples are of the chromel–Au(.07-at.% Fe) type. All data shown are corrected for the thermopower of gold.[19] The sample mounting was similar to that described above, using silver-paste for contacting, and in some cases (especially for TMTTF-DMTCNQ) Au evaporated contacts.

The optical properties were obtained from measurements of the polarized single-crystal reflectance. A single beam setup consisting of a Perkin-Elmer 98 prism monocromator with interchangeable KBr, NaCl, and SiO_2 prisms was used. A Perkin-Elmer gold wire grid on AgBr and a Glan-Thomson prism served as polarizers in the infrared and near-infrared spectral regions, respectively. Absolute values of reflectance were obtained by covering part of the crystals with an Al film and comparing the light intensities from covered and uncovered parts, correcting for the reflectance of the Al film.[20]

III. RESULTS

In Fig. 3 are shown typical normalized chain axis conductivities for the four alkyl substituted compounds as a function of temperature from 10 to 300 K. The overall behavior is very similar to

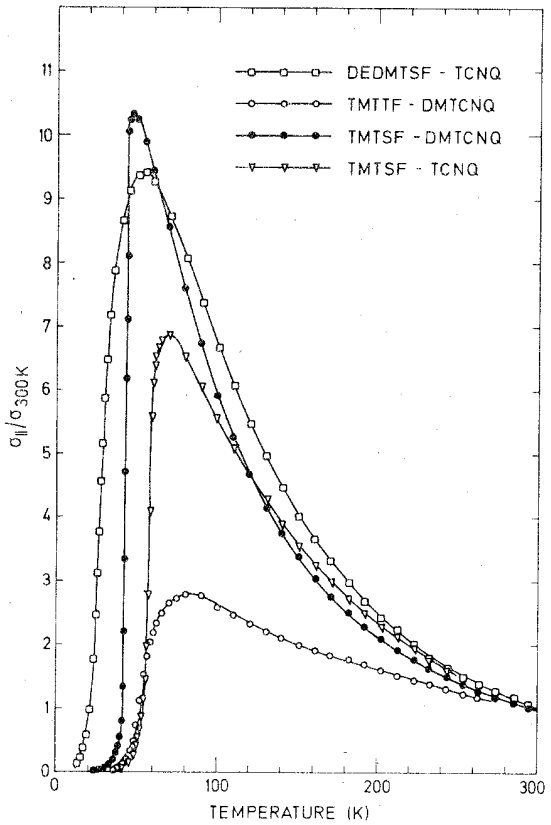

FIG. 3. Temperature dependence of stacking axis conductivities, normalized to room temperature values, for TMTSeF-TCNQ and DEDMTSeF-TCNQ, and for TMTSeF-DMTCNQ and TMTTF-DMTCNQ. Data points representing typical samples are shown.

what is usually found in this class of compounds: increasing conductivity with decreasing temperature, a relatively sharp maximum followed by a metal-insulator (M-I) transition below 100 K. The differing normalized peak values appear to be characteristic for the different materials (typical 10% scatter in σ_{max}/σ (300 K) from sample to sample of same material), although influence of imperfections characteristic for specific syntheses, purifications, and growth methods cannot be excluded.

Figure 4 shows the same data plotted as logσ vs $1/T$. From this activation plot absolute conductivity values can be read and details in the M-I transitions show up. Several interesting features become apparent: TMTSeF-TCNQ and TMTSeF-DMTCNQ have similar behavior, with a single sharp transition at 57 and 42 K, respectively. The transition temperatures are here taken to be the points of maximum slope in the activation plot. In contrast TMTTF-DMTCNQ shows two anomalies around 51 and 40 K. In this respect it is similar to other sulphur-containing compounds like TTF-TCNQ (Ref. 21) and HMTTF-TCNQ.[3] DEDMTSeF-TCNQ shows no transition at all, although the material gradually goes insulating at low temperatures. Thus, the material is still much different from HMTSeF-TCNQ (Ref. 5) and HMTSeF-11,11,12,12-tetracyanonaphto-2,6-quinodimethane(TNAP),[22] which retain their high metallic conductivities at low temperatures.

In order to compare the details in the transition region of the sulphur-selenium analogs TMTTF-DMTCNQ and TMTSeF-DMTCNQ, we directly measured the derivative dR/dT in these systems. In Fig. 5 the data are shown as $d(\ln R)/d(1/T)$, which extrapolates to the activation energy E_a/k_B at low temperatures. For both materials variations are found from sample to sample. The detailed behavior of the conductivity of TMTSeF-DMTCNQ is for example very sensitive to strain in and damage of the crystals. In damaged crystals the sharp anomaly generally splits up in two or three separate, but weaker anomalies, seemingly dependent on local strain fields, but most often found in a range of 3–4 K around 42 K. The results presented in Fig. 5 represents the sharpest anomalies observed, however, the intrinsic width of the transition may be even smaller, since the silver paint contacts unavoidably introduce some damage in otherwise perfect crystals. The results for the sulphur analog confirm the position of the two transitions. The broadening may be due to sample defects, but the fact that the anomalies are visible and reproducible does indicate that the crystals are of sufficient quality to give meaningful measurements of the transport properties.

We summarize the conductivity data in Table I, giving room-temperature values, normalized maximum values, transition temperatures, and activation energies for the semiconducting phases, as well as room-temperature anisotropy ratios where measured.

In addition to measurements on the pure materials we have also investigated a single doped system, TMTSeF-$(DMTCNQ)_{0.75}$ $(MeTCNQ)_{0.25}$, where the disorder introduced on the acceptor stacks should help understanding the roles played by the individual chains. MeTCNQ has previously been shown to have important effects on the electronic properties of similar systems.[23,24] The room-temperature conductivity is not much influenced, the reduction being of order 10%–20% in the doped system, presumably meaning that most of the conductivity is on the TMTSeF stacks in both materials. The change in the temperature dependence of the conductivity is more profound as shown in Fig. 6. The sharp transition at 42 K is completely smeared out and the low-temperature conductivity is more than one order of magnitude higher in the doped

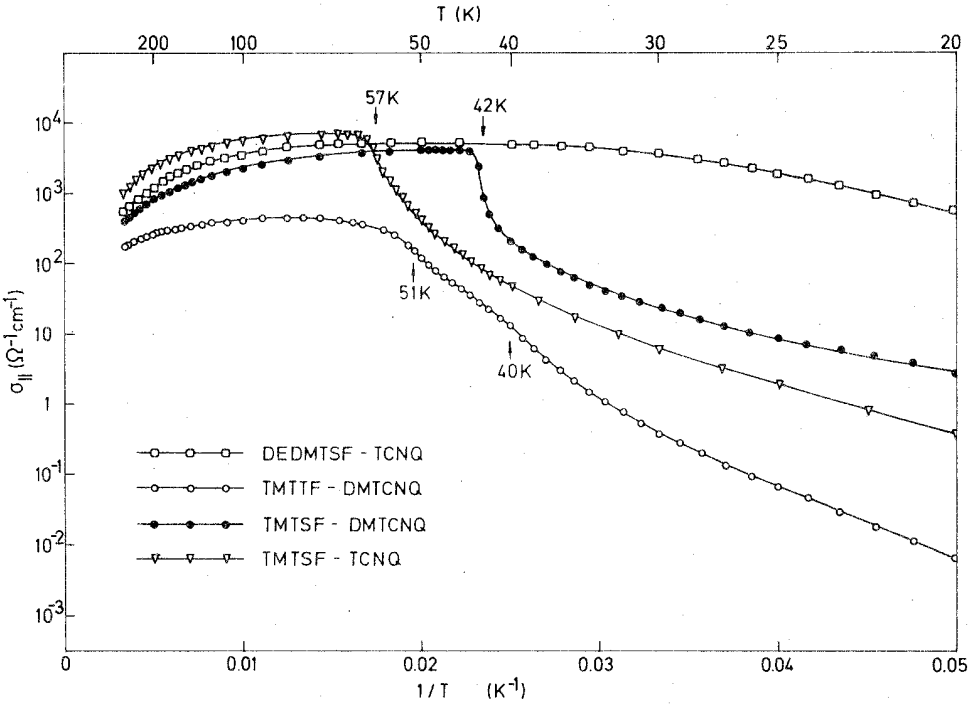

FIG. 4. Logarithm of conductivity vs inverse temperature for same samples as in Fig. 3.

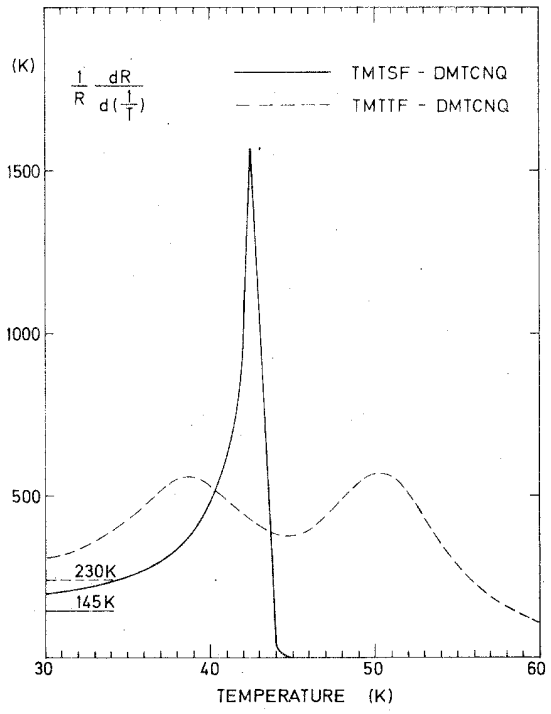

FIG. 5. Logarithmic derivative of resistance with respect to $1/T$ in the metal-insulator transition region for samples of TMTSeF-DMTCNQ and TMTTF-DMTCNQ.

compared to the undoped material.

Our complementary studies of the thermoelectric properties of the systems are presented in Figs. 7–10. Figure 7 shows the thermopower S plotted versus T in the range 20–300 K for all four compounds. $S(T)$ for the three Se containing salts are somewhat similar with linear segments above 200 K, nonlinear behavior down to the region of phase transitions, where sudden changes of slope are found at approximately the same temperatures as the anomalies in logσ (see Fig. 6). Interestingly, the thermopower of DEDMTSeF-TCNQ shows an anomaly at 28 K, the temperature where $\sigma(T)$ has its maximum slope (Table I). In spite of the missing anomaly in $\sigma(T)$, we may then take T_c = 28 K as the midpoint of a smeared transition.

The main feature of the high-temperature $S(T)$ of the three Se compounds is the rather low metallic-like values. In contrast $S(T)$ for TMTTF-DMTCNQ has a high nearly constant negative value from 100–300 K. The slight curvature seems to be reproducible, but some scatter is found from sample to sample. Together with the low absolute value of the room-temperature conductivity, the high value of S, and the absence of essential temperature dependence place TMTTF-DMTCNQ in a nonbandlike transport regime. Below 100 K $S(T)$ goes rapidly through zero to high positive

TABLE I. Conductivity data.

	σ_a(300 K) (Ω^{-1} cm^{-1})	σ_a/σ_b	σ_a/σ_c	T_{max} (K)	$\frac{\sigma_a(T_{max})}{\sigma_a(300\ K)}$	T_c (K)	E_a/k_B (K)
TMTSeF-TCNQ	1000	100	250	65	7	57	170
TMTSeF-DMTCNQ	400–600	200–300	200–300	47	10	42	145
TMTTF-DMTCNQ	120	···	···	80	3	40, 51	230
DEDMTSeF-TCNQ	500	···	···	55	9	28[a]	···

[a] Defined as the temperature of maximum slope in $\sigma(T)$.

values.

In Fig. 8 we show $S(T)$ plotted against $1/T$. This plot more clearly reveals the phase transition anomalies in TMTTF-DMTCNQ, seen at 50 K and at ~38 K. For this compound and for TMTSeF-DMTCNQ and TMTSeF-TCNQ semiconducting behavior is found at low temperatures. Clean linear segments are seen for the two TMTSeF salts. DEDMTSeF-TCNQ has a low value of S in the full range measured. This is consistent with the rather high conductivity in the low-temperature range (see Fig. 6).

In Figs. 9 and 10 we show the influence on S of doping into TMTSeF-DMTCNQ. Above 200 K, S is shifted upwards with a small constant amount. Below 200 K an additional contribution is found, evidently arising from the extra scattering from the MeTCNQ molecules. The small shift at high temperatures together with the positive sign in the metallic range again implies that TMTSeF-DMTCNQ is dominated by the TMTSeF stacks. This will be discussed in detail later in the paper.

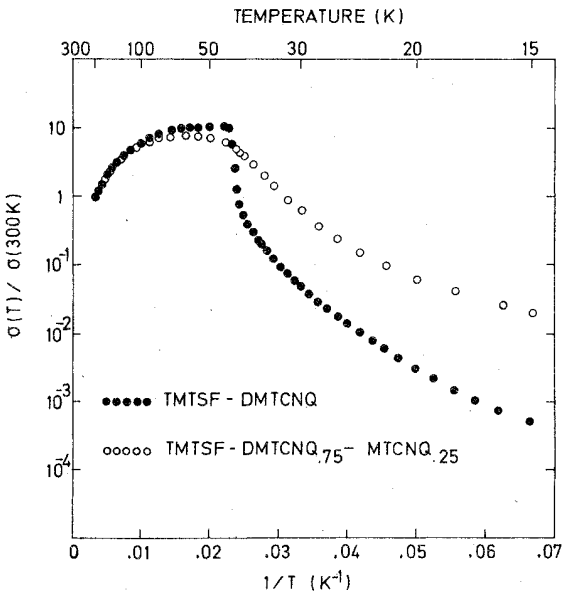

FIG. 6. Logarithm of conductivity vs inverse temperature for TMTSeF-DMTCNQ and for TMTSeF-DMTCNQ$_{0.75}$ (DMTCNQ)$_{0.75}$(MTCNQ)$_{0.25}$.

In order to achieve some independent information concerning band structure and carrier density we have finally performed an optical study of TMTSeF-TCNQ, TMTSeF-DMTCNQ, and TMTTF-DMTCNQ. In Fig. 11 we present the polarized single-crystal reflectance along the chains in the near infrared. The plasma edges are quite similar with deep minima at 8400, 8000, and 7500 cm^{-1}, respectively. The shifts are as one would expect from a simple qualitative estimate of

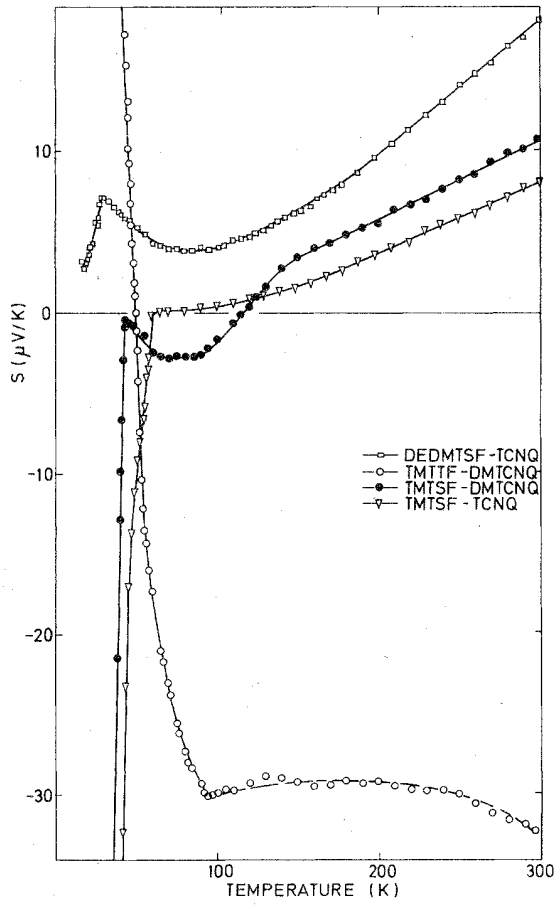

FIG. 7. Chain axis thermoelectric power vs temperature for TMTSeF-TCNQ and DEDMTSeF-TCNQ, and for TMTSeF-DMTCNQ and TMTTF-DMTCNQ. Data points for typical samples are shown.

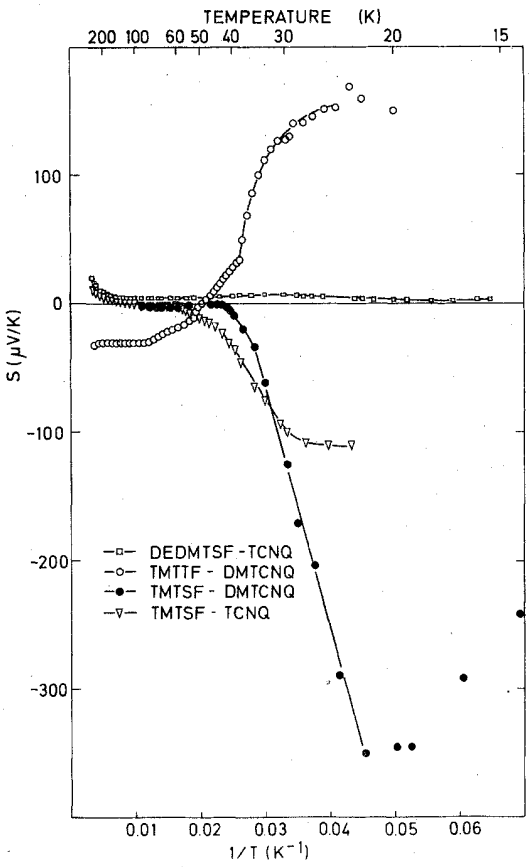

FIG. 8. Thermoelectric power vs inverse temperature for same samples as in Fig. 7.

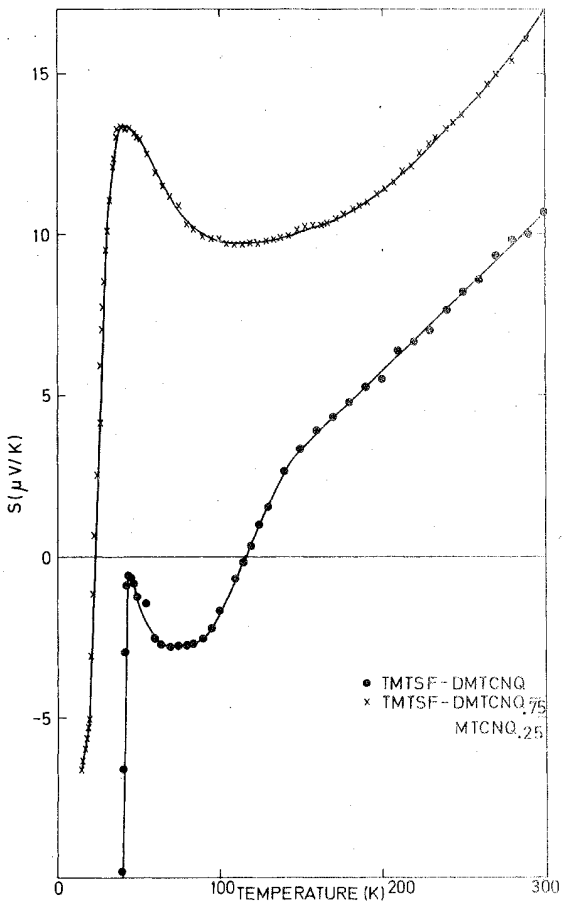

FIG. 9. Thermoelectric power vs temperature for TMTSeF-DMTCNQ and for TMTSeF-DMTCNQ$_{0.75}$ MTCNQ$_{0.25}$.

the overlaps, i.e., for the bandwidths: W(TMTSeF-TCNQ) > W(TMTSeF-DMTCNQ) > W(TMTTF)-DMTCNQ). Note that the well-resolved plasma minimum in TMTTF-DMTCNQ again implies acceptable sample quality. Above the plasma edges are seen transitions at 10 000–11 000 cm^{-1}, as usually found in TCNQ conductors.[25,26] One of the materials, TMTSeF-DMTCNQ, was available in reasonably sized crystals thus making possible a more complete study from the infrared (600 cm^{-1}) and throughout the visible (23 000 cm^{-1}) (see Fig. 12). The overall behavior is similar to what was found in, for example, TTF-TCNQ.[27,28] The high metallic reflectance in the infrared shows fine structure below 2000 cm^{-1}, presumably indicating coupling to the intramolecular vibration modes. The reflectance components perpendicular to the chain direction show rather dispersionless low values, slowly rising to transitions at higher energies.

IV. DISCUSSION

In the following we discuss the materials with special emphasis on the transport properties of the DMTCNQ salts. From a fundamental assumption of independent stacks at high temperatures we will try to separate the roles played by donor and acceptor stacks individually, and we demonstrate that the character of the transport on donor and acceptor stacks in TMTSeF-DMTCNQ is quite different. In addition, we present some estimates of the bandwidths and the degree of charge transfer derived from thermopower and optical data, and compare optical and dc conductivity. The last part of the discussion concerns the temperature region around and below the M-I transitions, where the transport data yield information about energy gaps and carrier sign.

A. Transport properties, high-temperature regime

In a first inspection of the conductivity values it is useful to calculate the electronic mean free paths. Assuming one carrier per molecule, equal conductivity on the two stacks, and using a tight-binding model

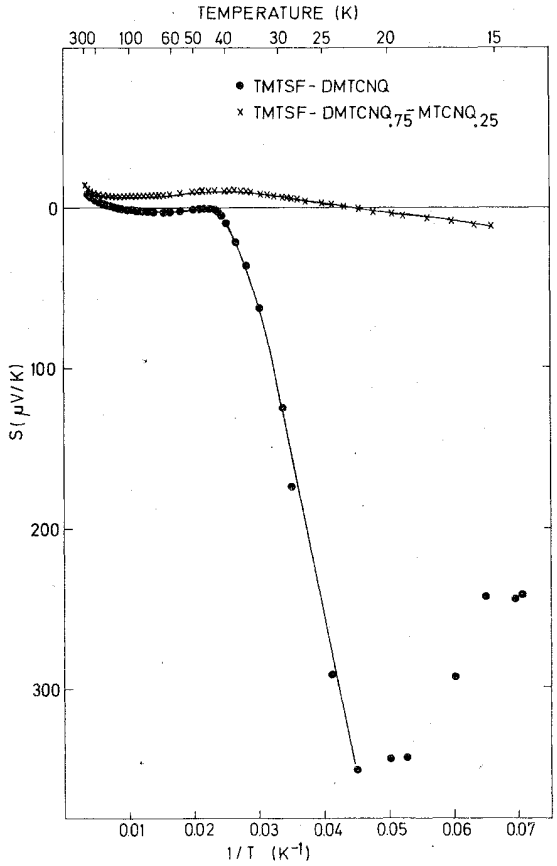

FIG. 10. Thermoelectric power vs inverse temperature for same samples as in Fig. 9.

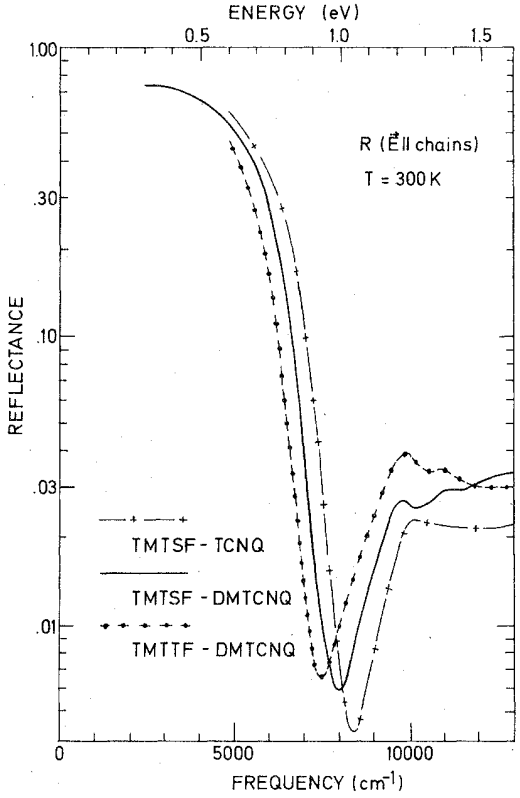

FIG. 11. Polarized stacking axis reflectance vs frequency from 5000–13 000 cm^{-1} for TMTSeF-TCNQ, TMTSeF-DMTCNQ, and TMTTF-DMTCNQ.

$$\Lambda/a \simeq \pi\hbar bc\sigma/4e^2a\,, \tag{1}$$

where Λ is the mean free path, a is the lattice constant in the stacking direction, b and c are the lattice constants perpendicular to the stacks, and σ is the conductivity. From the information in Table I and structural data we obtain in the conducting regime $\Lambda/a > 1.1$ for TMTSeF-TCNQ, $\Lambda/a > 0.7$ for TMTSeF-DMTCNQ, and $\Lambda/a > 0.15$ for TMTTF-DMTCNQ.

The numbers correspond to the room-temperature conductivities. Taking the temperature dependence into account places the first two compounds in the regime where $\Lambda/a \gg 1$, i.e., where band theory concepts are valid. For TMTTF-DMTCNQ, however, $\Lambda/a \ll 1$ at all temperatures and the transport can not be described properly by band theory. Rather the carriers are to be considered localized, and the transport may take place by activated hopping or by diffusion. The clear absence of an activated behavior then places TMTTF-DMTCNQ in the diffusion regime.

The next step is to decompose conductivity and thermopower into donor (D) and acceptor (A) contributions. The underlying assumption is that of independent bands, so one can write

$$\sigma = \sigma_D + \sigma_A\,, \tag{2}$$

$$S = (\sigma_D/\sigma)S_D + (\sigma_A/\sigma)S_A\,. \tag{3}$$

The assumption is primarily supported by the high anisotropies (see Table I), implying small interstack coupling. Typical transverse overlap integrals in TTF-TCNQ are estimated to be of order $t_\perp \sim 2$ meV,[29] and are probably smaller in the alkylated compounds. Thus, $k_BT \gg t_\perp$, and no coherent carrier exchange between chains is possible. The Coulomb interaction between carriers on different chains may be more important. However, if this interaction dominated the resistivity, one would expect a $\rho = AT$ law[30] instead of the T^2 behavior generally observed.[2]

Before attempting the decomposition, one may raise the question whether a specific kind of stack, say a TCNQ stack, will have the same intrinsic $\sigma(T)$ and $S(T)$ in different materials, provided the intrastack overlap and the charge transfer are unchanged. This clearly depends on what scattering mechanisms are important. If the scattering is mainly off high-energy intramolecular vibration modes,[31] then a TCNQ stack should always behave

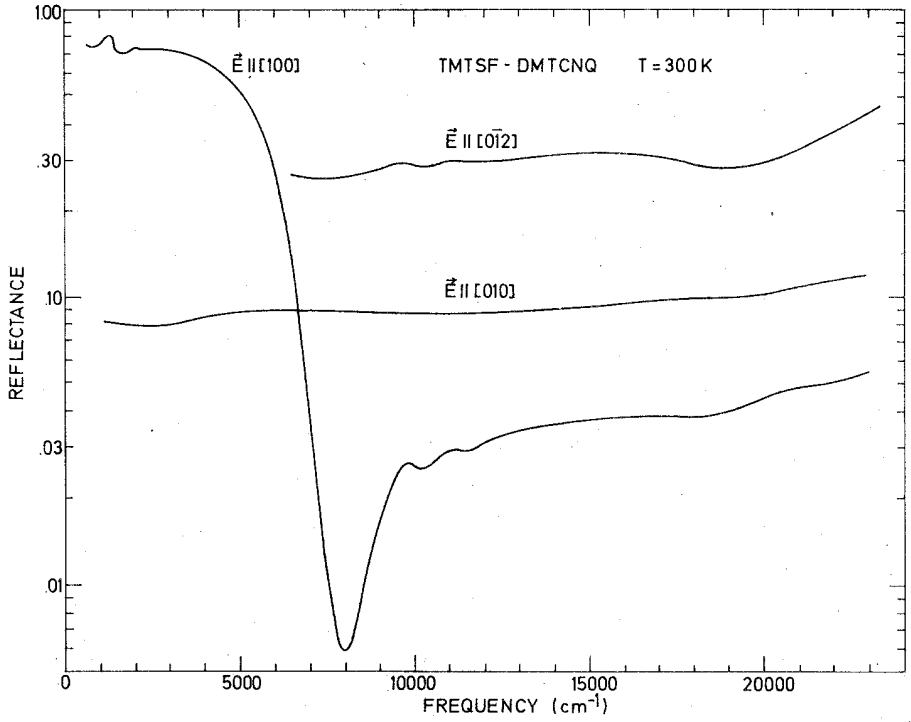

FIG. 12. Polarized reflectance vs frequency for TMTSeF-DMTCNQ. The stacking axis component, $\vec{E}\|[110]$, is shown from 600–23 000 cm^{-1}, the [010] component from 1000 to 23 000 cm^{-1}, and the [01$\bar{2}$] component from 6000 to 23 000 cm^{-1}.

in the same way. However, if movements of the molecules as a whole are involved in the electron scattering, the stack arrangement may be quite important for the frequencies of the modes: a closer packing generally gives rise to a stiffer lattice and vice versa. However, considering isostructural compounds such as the DMTCNQ salts. we do expect the DMTCNQ stacks to have approximately the same $\sigma(T)$and $S(T)$ in the two materials. Here we also assume approximately the same degree of charge transfer ρ in the two systems. This is supported by the experimental findings for other pairs of sulphur-selenium analogs. For TTF-TCNQ and TSeF-TCNQ ρ is[32] 0.59 and[33] 0.63, respectively, and for HMTTF- TCNQ and HMTSeF-TCNQ ρ is[34] 0.72 and[33] 0.74.

We therefore start our discussion with the DMTCNQ salts and begin with the low-mobility system TMTTF-DMTCNQ, which as stated above is best described as being in the diffusive regime. This is strongly corroborated by the size and temperature dependence of the thermopower S, which saturates to an almost constant, high value of -30 μV/K already at 100 K (see Fig. 7). If band behavior (coherent tunneling) was important, one would expect a dominating term in S proportional to T. On the contrary this experimental result suggests that the effective transfer integral $t_{\|} \ll k_B T$, that is $t_{\|}$ must be smaller than say 5 meV. As will be discussed later such small effective transfer integrals are possible, due to formation of small polarons.

The temperature dependence of the conductivity (Fig. 3) is weaker than observed in the majority of TTF-TCNQ derivatives. If we write $\rho(T) = \rho_0 + A T^{\lambda}$ we find a temperature-dependent λ going from approximately 2 at 300 K to 1 at 100–150 K.

In a simple treatment of diffusion in a system of noninteracting particles, the mobility is given by the Einstein relation,

$$\mu = eD/k_B T , \tag{4}$$

where D is the diffusion constant, which in the case of phonon-driven diffusion can be expressed

$$D = 2a^2 \nu_{ph} P , \tag{5}$$

a is the lattice constant, ν_{ph} the frequency of the driving phonon, and P is the probability for tunneling each time the levels on neighboring sites become degenerate. Equation (5) is easily derived from the diffusion expression for the mean-square displacement of a particle

$$\langle x^2 \rangle = 2Dt . \tag{6}$$

At low temperatures $P \to 1$ and the band regime is approached. At high temperatures $P \propto t_{\|}/\Delta$, where $t_{\|}$ is the transfer integral at $T = 0$ and Δ is the amplitude of the energy level modulation, caused

by the electron-phonon coupling. $\Delta^2 \propto T$ from Boltzmann statistics, consequently, we expect a $T^{-3/2}$ dependence of the mobility for $200 < T < 300$ K. The $1/T$ dependence seen at lower temperatures may indicate an approach to band behavior. To confirm this we estimate the value of P assuming a phonon frequency of order the Debye frequency in for example TTF-TCNQ,[35] $\nu_{ph} \simeq 2 \times 10^{12}$ sec^{-1}. One finds $P \sim 0.9$ at 300 K, thus verifying that TMTTF-DMTCNQ is close to the crossover regime between diffusion and band transport.

The next question is whether the conductivity is equally distributed on donor and acceptor stacks or whether one set of stacks dominates. The negative sign of thermopower suggests that the conductivity is electronlike and since the charge transfer in these salts is always found to be less than one, the main part of the conductivity most likely resides on the DMTCNQ stacks.

Let us for the moment assume that all the conductivity is on the DMTCNQ stacks. Then the thermopower observed should be that of the acceptor stacks. This leads us to the TMTSeF-DMTCNQ system, where the high-temperature thermopower (Figs. 7 and 9) roughly can be written

$$S_{\text{TMTSeF-DMTCNQ}} = S_0 + AT , \tag{7}$$

with $S_0 \simeq -4\,\mu$V/K and $A \simeq 0.05\ \mu$V/K^2. The thermopower of the doped system TMTSeF-$(\text{DMTCNQ})_{0.75}$ $(\text{MeTCNQ})_{0.25}$ (Fig. 9) is at high temperatures approximately AT. Here the acceptor stack conductivity is expected to be severely limited, so from Eq. (3), we conclude that

$$S_0 \simeq (\sigma_{\text{DMTCNQ}}/\sigma_{\text{total}})S_{\text{DMTCNQ}} . \tag{8}$$

From the conductivity values $\sigma_{\text{DMTCNQ}}/\sigma_{\text{total}}$ may be estimated to be about $100/500 = 0.2$, in qualitative agreement with $S_0/S_{\text{DMTCNQ}} = (-4\ \mu\text{V/K})/(-30\ \mu\text{V/K}) = 0.13$.

Hence, in our model the conductivity and thermopower data indicate that the conductivity on the DMTCNQ chains is diffusive and low, while on the TMTSeF chains it is rather high and in the band conduction regime. We note that this decomposition in TMTSeF-DMTCNQ confirms our earlier assumption, that the DMTCNQ stacks dominate in TMTTF-DMTCNQ. Thus, the TMTTF chains must have a rather low conductivity, presumably smaller than 30 Ω^{-1} cm^{-1}.

The accuracy of the absolute conductivity values does not allow us to perform a quantitative decomposition, but the general features seem to be clear, and we can ask what information can be gained from the actual values of the thermopower S. For the DMTCNQ stack system where S saturates in the high-temperature range, S depends only on the number of carriers per site ρ, and on interactions stronger than $k_B T$.[36] For fermions with spin,

$$S(T \to \infty) = -(k_B/e)\ln[(2-\rho)/\rho] , \tag{9}$$

which with $S = -30\ \mu$V/K leads to $\rho = 0.83$. For fermions with spin and strong on-site repulsion (only one carrier per site allowed),

$$S(T \to \infty) = -(k_B/e)\ln[2(1-\rho)/\rho] , \tag{10}$$

leading to $\rho = 0.59$. The assumption here is that $S_{\text{DMTCNQ}} \simeq S_{\text{TMTTF-DMTCNQ}}$. The correction for the donor stacks must be so, that the intrinsic S_{DMTCNQ} is even lower than $-30\ \mu$V/K. This would make ρ lower, but as shown above such a correction is probably small. The indication is therefore, that $0.59 < \rho < 0.83$ in TMTTF-DMTCNQ in agreement with what is found in similar systems.

In TMTSeF-DMTCNQ we can analyze the TMTSeF thermopower, which is linear in temperature (down to 150 K), using the approximate value with correction for acceptor chain conductivity $S \simeq 0.06\ (\mu\text{V/K})T/K$. Within a band picture, S is given as[37]

$$S = -\frac{\pi^2 k_B^2 T}{3e}\left(\frac{\epsilon_k''}{(\epsilon_k')^2} + \frac{\tau'(\epsilon)}{\tau(\epsilon)}\right)_{\epsilon=\epsilon_F} . \tag{11}$$

Here ϵ_k is the electron energy for quantum number k, and $\tau(\epsilon)$ is the momentum relaxation time. $\tau'(\epsilon)/\tau(\epsilon)$ is normally small at high temperatures[38] and is in any case expected to be temperature dependent. The linear behavior observed suggests this term to be negligible and with a tight-binding band,

$$\epsilon_k = \tfrac{1}{2} W \cos ka , \tag{12}$$

W being the bandwidth, we obtain

$$S = \frac{2\pi^2}{3} \frac{k_B}{e} \frac{\cos(\frac{1}{2}\rho\pi)}{\sin^2(\frac{1}{2}\rho\pi)} \frac{k_B T}{W} , \tag{13}$$

where ρ is the number of holes per site, equal to the charge transfer. The experimental value allows us to calculate the quantity

$$W \sin^2(\tfrac{1}{2}\rho\pi)/\cos(\tfrac{1}{2}\rho\pi) = 0.8\ \text{eV} .$$

The optical data shows that $W_{\text{TMTSeF}} < 0.56$ eV, thus, giving us a lower limit on ρ, $\rho > 0.65$. W in (13) is almost certainly smaller than the optically observed bandwidth due to small polaron effects, so ρ is likely to be somewhat higher. These results will be further confirmed in the discussion of the optical data, but before turning to this let us shortly comment on the two other systems: TMTSeF-TCNQ and DEDMTSeF-TCNQ.

σ(300 K) is ~1000 Ω^{-1} cm^{-1} for TMTSeF-TCNQ and ~500 Ω^{-1} cm^{-1} for DEDMTSeF-TCNQ. We attribute the main part of this difference to changes in bandwidths due to the substitution of the rather

bulky ethyl groups. The chain axis lattice constant in the latter salt is 4.0 Å,[10] as compared to[9] 3.88 Å for the first. Only inadequate optical data has been obtained for DEDMTSeF-TCNQ, so no independent information on bandwidth is available.

The thermopower in both systems is small and positive, approximately linear in T at high temperatures. The sign suggests donor stack dominance in the conductivity. The higher value of S for DEDMTSeF-TCNQ can again be due to a smaller bandwidth [see Eq. (13)], but S is also very sensitive to a possible difference in charge transfer. For these materials we must also consider the acceptor stack contributions. The TCNQ stack conductivity can not be expected to be negligible and a negative term in S must be present. In both compounds the linear segments of S extrapolates to negative values at low T. Such behavior can be qualitatively understood as resulting from different temperature dependences of donor and acceptor stack conductivities, even when S_D and S_A are both proportional to T. To explain the data, the TCNQ stack conductivity must be assumed to rise faster as the temperature is lowered than the donor stack conductivity, [see Eq. (3)]. Some support for such an interpretation comes from the fact that the normalized conductivity in the salt TMTTF-TCNQ rises more rapidly[2] [$\sigma_{max}/\sigma(300\ K) \sim 15$] than in TMTSeF-TCNQ. Since we expect the TMTTF stack to have a small conductivity the mobility on the TCNQ stacks should then rise faster than the mobility on the TMTSeF stacks, giving a qualitative explanation for the observed thermopower. This comparison is not immediately allowable since the sulphur and selenium analogs are not isostructural.[9,39] The stacking pattern is, however, rather similar. Further progress in decomposing the donor and acceptor stack contributions must await measurements of thermopower in the sulphur analogs. These are unfortunately not easily obtainable as single crystals.

B. Optical properties

Now let us consider the transport properties in the light of the optical data. The dominant feature in the reflectance component along the chain axis (Fig. 11) is the strong drop in the near infrared. This edge moves slightly from compound to compound, but never more than 10%–20%. From the comparable low-frequency properties we also expect more or less the same behavior in the intermediate ir. We can then use the TMTSeF-DMTCNQ system as representative (Fig. 12). The reflectance R is quite high throughout the ir, but at lower frequencies R has several minima indicating deviations from the smooth metallic behavior. These are easier to characterize in the optical conductivity $\sigma_1(\omega)$, which can be found by Kramers-Kronig transforming the reflectance data. The extrapolations used include a Hagen-Rubens continuation to zero frequency and a ω^{-2} fall off at high frequencies. $\sigma_1(\omega)$ is shown in Fig. 13 (solid line). The strong deviations from a monotonic behavior is found in the range below ~2000 cm^{-1}, where also most of the phonons are located. The dip at 1500 cm^{-1} and the fall off from 1000 cm^{-1} in the far infrared therefore presumably is due to effects of the electron-phonon coupling. Quite similar effects are found in TTF-TCNQ,[28] and HMTSeF-TCNQ.[40]

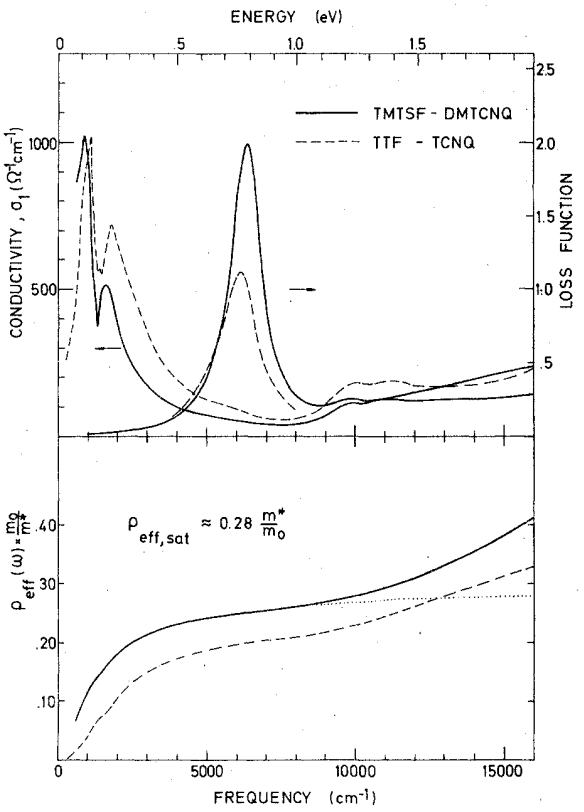

FIG. 13. Results of Kramers-Kronig analysis of the data shown in Fig. 12. The upper part of the figure shows the optical conductivity (solid line) for TMTSeF-DMTCNQ. In the region of the plasma edge is also shown the energy-loss function $-\mathrm{Im}(1/\tilde{\epsilon})$. The lower part of the figure shows the sum rule calculation, Eq. (14). Data are shown for TTF-TCNQ (Ref. 28) for comparison.

We may now take the view that although $\sigma_1(\omega)$ cannot be continued monotonically from the near ir to dc, the near infrared behavior does give information about carrier density and band structure, but on a time scale short compared to all lattice and molecular vibrations.

The proper way of analyzing the data is to in-

tegrate the oscillator strength,

$$\rho_{\mathrm{eff}}(\omega)\ \frac{m_0}{m^*} = \frac{2}{\pi}\ \frac{V_c m_0}{e^2}\int_0^{\omega} \sigma(\omega')\,d\omega' \ . \qquad (14)$$

Here $\rho_{\mathrm{eff}}(\omega)$ is the effective number of carriers per average molecular volume V_c, participating in the optical transitions up to frequency ω. m^* is an optical effective mass. The result of the calculation is shown in Fig. 13 (bottom, solid line). The curve is easily extrapolated to a saturation value of about 0.28, which corresponds to an unscreened plasma frequency

$$\omega_p = (\rho e^2/V_c\,\epsilon_0 m^*)^{1/2} = 9200\ \mathrm{cm}^{-1} .$$

Another method which can be used if only data around the plasma edge is available, is to find the plasmon frequency Ω_p from the zero crossing of ϵ_1, or from the peak in the loss function, $-\mathrm{Im}(1/\tilde{\epsilon})$ (see Fig. 13). We note that this position is quite insensitive to details in the choice of extrapolations in the Kramers-Kronig scheme. Ω_p can be interpreted as the screened plasma frequency

$$\tilde{\omega}_p = (\rho e^2/V_c\,\epsilon_{\mathrm{core}}\,\epsilon_0 m^*)^{1/2} \simeq \Omega_p = 6260\ \mathrm{cm}^{-1} ,$$

where ϵ_{core} is the background dielectric constant. For the TCNQ salts the following approximate empirical expression holds for ϵ_{core}[41]:

$$\epsilon_{\mathrm{core}} \simeq [1 + (320\ \text{Å}^3)/V_c] . \qquad (15)$$

Using this we find $\omega_p = (\epsilon_{\mathrm{core}})^{1/2}\tilde{\omega}_p = 9030\ \mathrm{cm}^{-1}$ in reasonable agreement with the result of the sum-rule calculation.

Neglecting for a moment the deviations from Drude behavior at low frequencies, we can use ω_p and the optical relaxation rate Γ to find the corresponding dc conductivity. Γ is the halfwidth of the plasmon peak in the loss function $\Gamma \simeq 1280\ \mathrm{cm}^{-1}$. Note that Γ derived from the fall off in $\sigma_1(\omega)$ is approximately the same, confirming the Drude behavior in the range from 2000 to 8000 cm^{-1}. Then

$$\sigma_{\mathrm{optical}}(\omega = 0) = \epsilon_0\omega_p^2/\Gamma = 1100\ \Omega^{-1}\mathrm{cm}^{-1} :$$

a factor of 2 above the observed dc conductivity. This confirms the observation made for TTF-TCNQ,[42] that the dc and optical conductivities are not immediately comparable.

Another important piece of information obtainable from the optical properties concerns the bandwidth and carrier density. Within a self-consistent-field approximation, neglecting local-field effects, the intraband contribution to $\epsilon(\omega)$ can be written[43]

$$\Delta\epsilon_{\mathrm{intra}} = -\frac{e^2}{\epsilon_0\omega^2}\sum_k f(\epsilon_k)\left(\frac{1}{\hbar^2}\ \frac{\partial^2\epsilon}{\partial k^2}\right), \qquad (16)$$

where $f(\epsilon)$ is the occupation number for a state with energy ϵ. The sum runs over all states in the band. In this case there are two partly filled bands, which in the tight-binding approximation and assuming an inverted band structure[44] can be written

$$\epsilon_A(k) = -\tfrac{1}{2}W_A\cos ka, \quad \epsilon_D(k) = \epsilon_{D0} + \tfrac{1}{2}W_D\cos ka . \qquad (17)$$

W_A and W_D are the individual acceptor and donor bandwidths, and ϵ_{D0} is a constant. The Fermi wave vector for the two bands is the same $k_F = \rho\pi/2a$. Inserting (17) in (16) yields in the limit $k_B T \ll W_A, W_D$:

$$\Delta\epsilon_{\mathrm{intra}} = -\frac{\omega_p^2}{\omega^2},$$

$$\omega_p^2 = \frac{e^2a^2\sin(\frac{1}{2}\rho\pi)}{\pi\epsilon_0\hbar^2 V_c}\left(\frac{W_A + W_D}{2}\right) \ . \qquad (18)$$

Hence, the quantity which can be determined is in this model $W\sin(\frac{1}{2}\rho\pi)$, where $W = \frac{1}{2}(W_A + W_D)$.

In Table II we have collated the resulting data for TMTSeF-DMTCNQ, TMTTF-DMTCNQ, and TMTSeF-TCNQ. Data for TTF-TCNQ are included for comparison. Several conclusions can be drawn from our model. In TTF-TCNQ the degree of charge transfer $\rho = 0.59$.[32] This results in $W(\mathrm{TTF\text{-}TCNQ}) = 0.43$ eV. Since it is inconceivable that the bandwidth of the methylated TMTTF-DMTCNQ should be larger than that, we can set a lower limit on ρ, $\rho(\mathrm{TMTTF\text{-}DMTCNQ}) > 0.66$. Actually, one might be tempted to estimate the reduction in bandwidth going from TCNQ to DMTCNQ from the data on the TMTSeF salts. The result is

$$\Delta W_A = W(\mathrm{TCNQ}) - W(\mathrm{DMTCNQ})$$
$$= 2\left(\frac{0.47}{\sin(\frac{1}{2}\rho_1\pi)} - \frac{0.42}{\sin(\frac{1}{2}\rho_2\pi)}\right)\mathrm{eV} .$$

TABLE II. Optical parameters.

	$\Omega_p(\mathrm{cm}^{-1})$	$\omega_p(\mathrm{cm}^{-1})$	$\Gamma(\mathrm{cm}^{-1})$	$\sigma_{\mathrm{opt}}(\omega=0)$ $(\Omega^{-1}\mathrm{cm}^{-1})$	$W\sin(\frac{1}{2}\rho\pi)$ (eV)
TTF-TCNQ	5930	9420	1640	900	0.34
TMTSeF-TCNQ	6700	9880	1270	1300	0.47
TMTSeF-DMTCNQ	6260	9030	1280	1100	0.42
TMTTF-DMTCNQ	5930	8580	1490	800	0.37

Assuming equal charge transfer in the two leads to $\Delta W_A \simeq 0.10$ eV, which would give ρ [TMTT(Se)F-DMTCNQ] $\simeq 1$. However, even rather small differences in ρ for the two TMTSeF salts will upset this estimate. Anyway, the optical data seems to give a rather high value of ρ in the DMTCNQ complexes. This is consistent with the independent estimates from the dc transport data, as discussed earlier. Assuming a high ρ in the two DMTCNQ salts gives a difference in donor band-widths $\Delta W_D = W(\text{TMTSeF}) - W(\text{TMTTF}) = 2(0.42-0.37)$ eV $= 0.10$ eV, which is considerable since W(TMTTF) in itself is probably rather small $\sim 0.2-0.3$ eV.

The previously used estimate of W(TMTSeF) comes about as follows: Since TMTTF-DMTCNQ is dominated by the acceptor chains it is reasonable to believe $W(\text{TMTTF}) \leq W(\text{DMTCNQ})$. Consequently, $\frac{1}{2}\sin(\frac{1}{2}\rho\pi)W(\text{DMTCNQ}) \geq 0.18$ eV and $W(\text{TMTSeF}) \leq 2(0.42-0.18)/\sin(\frac{1}{2}\rho\pi)$ eV $= 0.48/\sin(\frac{1}{2}\rho\pi)$ eV. With $\rho \geq 0.66$ (see above) we have $W(\text{TMTSeF}) \leq 0.56$ eV.

The inferred dc conductivities are significantly higher than the actual values for the DMTCNQ compounds, but comparable for TMTSeF-TCNQ (see Tables I and II). Also note that the optical scattering rates are comparable for all materials, somewhat smaller for Se compounds compared to S compounds. So it seems that the dominating scattering mechanism responsible for absorption in the near infrared is of about equal strength in all the organic conductors, while quite significant differences are found at low frequencies.

The actual mechanism of absorption in these materials in the plasmon region is unknown. Inelastic electron scattering data on TTF-TCNQ,[45] indicate the absence of Landau damping of the plasmons, and there seems to be no allowed single-particle excitations in this range beyond the conduction bandwidth. The absence of a low-lying higher band is also confirmed by the absence of structure in $\sigma_1(\omega)$, i.e., by the constant relaxation rate. Therefore, the final states in the optical absorption processes are presumably in the conduction bands and the excess energy is most likely disposed of by multiple phonon emission. A variety of high-energy optical vibration modes are known to couple strongly to the conduction electrons in these materials[46] and furthermore we expect coupling strengths and mode frequencies to be comparable in all materials. Some change is of course expected going from a sulphur to a selenium compound, but addition of methyl groups will probably not change coupling strengths and mode frequencies very much for the more important vibrations (like the C=C ring stretch[46] in TCNQ.)

The higher-order absorption processes must involve intermediate states in higher bands, so matrix elements of the electron-phonon interaction between states in different bands will enter. Thus, the optical lifetime and the dc lifetime may have quite different origins and no simple relation between σ_{dc} and $\sigma_{optical}$ is expected.

C. Review of conductivity theories

This leads us to discuss the origin of the dc conductivity in the materials. A number of different interpretations of the unusual temperature dependence of ρ in TTF-TCNQ have been put forward. The resistivity is usually fitted to the $\rho_0 + AT^\lambda$ form, where λ is found to be ~2.3 if the fit is made over the full temperature region. However, more detailed fits shows that λ is quite temperature dependent.[47] Also in about 10% of TTF-TCNQ crystals from carefully prepared batches unusual high normalized conductivity ratios are found.[48] This has led to the suggestion[1,49] that the conductivity at least in the neighborhood of the maximum should be dominated by collective mode transport, i.e., the so-called Peierls-Frohlich conductivity.[50] At temperatures above approximately 150 K a single-particle description may be more appropriate as, for example, evidenced in the thermopower which is linear in the high-temperature regime.[37,51] The same seems to be true for the materials we have investigated. So one is looking for a mechanism which can give a $\sim T^2$ contribution to the resistivity.

Recently, Cooper and Jerome[52] suggested that $\rho(T)$ measured at ambient pressure should be corrected for the thermal expansion using data on the pressure dependence of $\rho(T)$. They find for TTF-TCNQ a resistivity at constant volume proportional to T, and Jerome[53] has further suggested that this T dependence and the large pressure dependence can be understood as resulting from electron-spin wave collisions in one dimension.

Another explanation which employs the one-dimensional character of the materials is the dynamic disorder picture by Cohen and coworkers.[54] Here the transport is by diffusion through one-dimensional states localized by thermal disorder. The localization length is shown to vary as $1/T$ and for a system with bandwidth $W \gg k_B T$ this leads to a $1/T^2$ law in the conductivity.

For some time the only single-particle process proposed was electron-electron scattering.[55] However, for temperatures where $k_B T \gg t_\perp$, the contributions to ρ from this process goes as T^1,[30] and not as in two- and three-dimensional systems as T^2.

Recently, two different electron-phonon scattering processes have been suggested. The first by Conwell[31] is based on scattering from high-energy intramolecular vibration modes and does

not give an exact T^{λ} behavior, but still a variation rather close to $T^{2.3}$. The second by Gutfreund and Weger[56] explains the $\sim T^2$ law as arising from second-order electron-libron coupling. The librons involve the rotational degree of freedom of the molecules, and the important motion corresponds to rotations approximately in the molecular plane.

In principle, both mechanisms contribute, and currently it is not clear if one is dominating. It would seem easier to explain the big differences in absolute values of conductivities between different materials from the latter mechanism. Interestingly, the electron-libron scattering model also provides us with a simple explanation for the degraded conductivity on the DMTCNQ stacks. In TCNQ stacks in, for example, TTF-TCNQ, the overlap is symmetric about the long axis of the molecule.[57] Consequently, first-order coupling between electrons and librons are forbidden. In DMTCNQ stacks the overlap is quite asymmetric (Fig. 2) such that this argument breaks down. One may argue that the equilibrium position of the molecules must be such that the overlap is maximum, but this is only true for the total binding energy from all occupied bonding π orbitals. Therefore, a first-order contribution to the modulation of the conduction-band transfer integral is conceivable, and such an effect is on general grounds expected to be strong.

Experimentally, we found the electrons to be effectively localized and the transport to take place by diffusion. It is not clear how the transport should be described in detail. In a coupled electron-phonon system with increasing interaction strength, one expects eventually the formation of small polarons,[58] i.e., carriers followed by their induced polarization cloud of phonons. The small-polaron limit corresponds to this cloud being comparable to a lattice constant. Important effects of small-polaron formation are exponential band narrowing and a reduction in effective on-site Coulomb repulsion.[59] These effects may qualitatively explain the anomalous thermopower found in TMTTF-DMTCNQ. The band narrowing, giving $t_{\parallel} < k_B T$, is not effective at optical frequencies, well above all important phonon frequencies. The apparent controversy between dc and optical bandwidths may therefore be resolved in this way.

The concept of small polarons was developed for small carrier concentrations in polar crystals and detailed theories for the transport properties at high densities are not known to us. Another approach may be through the dynamic disorder picture[54] in the limit where the localization length approaches one lattice constant. With these remarks of more speculative nature we will leave the high-temperature regime and turn to the behavior around and below the metal-insulator transitions.

D. Transport properties, transition region and low-temperature regime

In the low-temperature range the double-chain compounds in question show spectacular effects of the one-dimensional instabilities inherent in these highly anisotropic systems. Roughly what is believed to happen is the development of a giant $2k_F$ Kohn anomaly in one or more phonon branch. The corresponding $2k_F$ charge-density waves lock in to the lattice at the temperature T_c, which then represents a normal $3d$ phase transition. Above T_c we have a metallic state. Below T_c an energy gap opens at the Fermi level creating a small band-gap semiconductor. The transport properties are further complicated by the possibility of contributions to the conductivity from the pinned charge-density waves below T_c. Above T_c fluctuation effects might be important in the sense that the mean-field scaling temperature could be much higher than the observed transition temperature T_c. In that case the mobility could be enhanced by the $2k_F$ scattering, i.e., we have a charge-density wave contribution to the conductivity.[1] The opposite view is that the mean-field temperature is very close to T_c,[60] just a few degrees Kelvin higher. In that case the conductivity should essentially be single-particle-like above T_c.

In the present paper we will take the view that the deviations from linearity in the thermopower identifies the regime where fluctuations are important for the transport properties. Other explanations for the nonideal behavior may be visualized. The derivative term $\tau'(E)/\tau(E)$ in the band expression for the thermopower may be important, or σ_A/σ_D could be temperature dependent and according to Eq. (3) give an apparent nonideal behavior.

Below T_c we have a semiconducting state, where the conducitivity is approximately described by $\sigma(T) = \sigma_0 \exp(-E_a/k_B T)$. The simplest interpretation of E_a is that $E_a = \frac{1}{2} E_g$, E_g being the semiconducting energy gap. Since there are two sets of chains we expect two such contributions with different E_a's. The thermopower for a semiconductor is given by[61]

$$S = -(k_B/e)[(b-1)/(b+1)(E_g/2k_B T) + A]\,. \quad (19)$$

Here b is the ratio of electron to hole mobility, and A is essentially temperature independent. Again in an independent chain model two contributions are weighted with their respective conductivities. Some support for such a model is given

by the rather general observation that S below T_c has the opposite sign of S at high temperatures. In (19) b is expected to be larger than 1 in an acceptor band with $\rho<1$ ($S<0$) and smaller than 1 in a donor band ($S>0$). If a certain band is dominating at high temperature the interactions will tend to be stronger here, and the bigger energy gap will appear in this band. At low temperatures the band with the smaller gap will dominate the conductivity and therefore the thermopower. Hence, the opposite signs of S (low T) and S (high T). Exceptions from this rule can be anticipated in systems with comparable interaction strengths in the two subsystems.

Now let us discuss the materials one by one again starting with TMTTF-DMTCNQ (see Figs. 3, 4, 7, and 8). In this low-mobility system the thermopower is constant ~-30 μV/K down to 100 K. Below 100 K, $|S|$ decreases reaching zero at 50 K, where an anomaly is seen in σ as well as S. The rather narrow temperature regime, where S goes to zero is consistent with the interpretation developed for the transport. The thermal disorder giving the diffusive character of the conduction process does not allow development of any order until at a fairly low temperature. But as band behavior is approached the $2k_F$ instability develops and the strong coupling in the system gives a relatively high T_c, despite the rather narrow bands. Presumably the order is primarily developing on the acceptor chains like in TTF-TCNQ,[62] so that the ordering is not complete until around 40 K where a second anomaly is seen in S and σ. This behavior may be analogous to that of TTF-TCNQ,[62] and HMTTF-TCNQ,[3] where split-up transitions are seen as well. In the low-temperature range, the activation energy from $\sigma(T)$ is ~230 K. No well-defined activation energy can be derived from $S(T)$.

The behavior of the selenium analog is drastically different. The positive sign of S at high temperature indicates dominating donor chains. Deviations from linear behavior are seen below 150 K. Let us discuss these in the light of the decomposition proposed above. With an unchanged acceptor chain contribution, S(TMTSeF) seems to drop to near zero at 80 K and from 80 K to T_c = 42 K, S(DMTCNQ) goes to zero and the transition takes place. This could indicate a broad temperature range $42<T<150$ K, over which correlations are developing on the donor chains. A tempting explanation for vanishing thermopower is that the current is carried collectively. Alternatively in a single-particle picture, the interpretation would be based on a strong temperature and energy dependence of τ. However, the proposed decomposition may not be valid in this range, and the explanation could as well be a temperature-dependent σ_A/σ_D. Below T_c there are other interesting details in S. Down to 35 K there is a linear segment corresponding to an activation energy $E_a/k_B = 39$ K. Between 22 and 35 K S is again linear in $1/T$, while at lower temperatures S is presumably dominated by impurity effects. The activation energy in the low-temperature range is 116 K. Both the E_a's are smaller than $E_a/k_B \approx 145$ K derived from conductivity. This is in agreement with the expectation from Eq. (19). In the doped system TMTSeF-$(DMTCNQ)_{0.75}$ $(MeTCNQ)_{0.25}$ (Figs. 6, 9, and 10) $S(T)$ deviates from simple band behavior below 200 K. This is obviously an effect of the introduced disorder. We believe the MeTCNQ molecules destroy the conductivity on the DMTCNQ chains and also via their randomly oriented dipole fields influence the donor stacks. As expected the turn up of S starts exactly where the normalized conductivity in the doped system starts falling below that of the undoped system (see Fig. 6). The positive sign of ΔS corresponds for a donor chain and within a band picture to an increase in lifetime with increasing velocity, which is exactly what is expected for impurity scattering.

At lower temperatures the effect on the conductivity is to strongly smear out the transition, and throughout the low-temperature regime the normalized conductivity is approximately one order of magnitude larger than that of the pure compound. Apparently the disorder creates considerable band tailing into the gaps. As evidenced from the thermopower the carrier sign eventually changes as in the undoped system, but at these low temperatures effects of other impurities may be important as well.

We will not comment much further on the TMTSeF-TCNQ system. S is small and shows no unusual behavior above T_c. Below T_c, S is negative, and two linear segments are found in the $1/T$ plot (Fig. 8). The corresponding activation energies are $E_a/k_B \simeq 37$ K down to 45 K and $E_a/k_B \simeq 90$ K below 45 K. In this respect TMTSeF-TCNQ and TMTSeF-DMTCNQ are quite similar. E_a/k_B from $\sigma(T)$ is $\simeq 170$ K.

The most interesting feature in DEDMTSeF-TCNQ is the total smearing of $\sigma(T)$ in the transition region. In view of experiences from other systems and from the doped system presented in this work, we interpret this smearing as arising from static disorder in the material, probably from random stacking of the *cis* and *trans* forms of DEDMTSeF. This is confirmed by the low-temperature thermopower (Fig. 8) which qualitatively behaves as in the doped system (see above). We interpret the upturn of S below 80 K to be due to scattering from the disorder potential.

Below 28 K S falls again, presumably because of an increased acceptor stack contribution to the transport relative to the donor stack contribution.

V. SUMMARY AND CONCLUSIONS

We have presented the results of an experimental study of the transport properties of a group of quasi-one-dimensional organic conductors closely related to TTF-TCNQ. In all materials we find metal-insulator transitions in the range below 60 K. It has been demonstrated that various kinds of disorder smear the transition.

Measurements of thermoelectric power indicate donor-stack dominance in all selenium compounds and acceptor stack dominance in the only sulphur system investigated. Using isostructural sulphur and selenium containing materials as well as doping into specific stacks we have proposed a decomposition of the transport properties into donor and acceptor contributions for the system TMTSeF-DMTCNQ. The result is metallic conductivity on the TMTSeF stacks and low diffusive conductivity on the DMTCNQ stacks, which tentatively is linked to the theory of Gutfreund and Weger[56] on electron-libron scattering. The optical properties have been found to be quite similar for all the materials in contrast to the dc transport properties, but small shifts in the plasma edge give important information on changes in bandwidths.

In conclusion, we have found the combination of molecular engineering and physical measurements, such as conductivity, thermopower, and optical properties, to be quite powerful in attempting to understand the role of individual molecular stacks in the interesting group of highly conducting, organic charge transfer salts surrounding TTF-TCNQ.

ACKNOWLEDGMENTS

We are grateful to Dr. James E. Weidenborner for doing the powder diffraction analysis on TMTTF-DMTCNQ. We also thank Dr. H. Soling, Dr. G. Rindorf, and Dr. N. Thorup for advice on sample etching and especially for their valuable assistance in all questions concerning crystal structure and orientations.

[1]A J. Heeger, *Chemistry and Physics of One-Dimensional Metals*, edited by H. J. Keller (Plenum, New York, 1977), p. 87.
[2]A. N. Bloch, T. F. Carruthers, T. O. Poehler, and D. O. Cowan, *Chemistry and Physics of One-Dimensional Metals*, edited by H. J. Keller (Plenum, New York, 1977), p. 47.
[3]R. L. Greene, J. J. Mayerle, R. Schumaker, G. Castro, P. M. Chaikin, S. Etemad, and S. J. LaPlaca, Solid State Commun. 20, 943 (1976).
[4]R. L. Friend, D. Jerome, J. M. Fabre, L. Giral, and K. Bechgaard, J. Phys. C 11, 263 (1978).
[5]A. N. Bloch, D. O. Cowan, K. Bechgaard, R. E. Pyle, R. H. Banks, and T. O. Poehler, Phys. Rev. Lett. 34, 1561 (1975).
[6]J. R. Andersen, C. S. Jacobsen, G. Rindorf, H. Soling, and K. Bechgaard, J. Chem. Soc. Chem. Commun. 883 (1975).
[7]J. R. Andersen, K. Bechgaard, C. S. Jacobsen, G. Rindorf, H. Soling, and N. Thorup, Acta Crystallogr. (to be published).
[8]J. E. Weidenborner (private communication).
[9]K. Bechgaard, T. J. Kistenmacher, A. N. Bloch, and D. O. Cowan, Acta Crystallogr. B 33, 417 (1977).
[10]G. Rindorf, H. Soling, and N. Thorup (private communication).
[11]R. E. Pyle, A. N. Bloch, D. O. Cowan, K. Bechgaard, T. O. Poehler, T. J. Kistenmacher, V. V. Walatka, R. Banks, W. Krug, and T. E. Phillips, Bull. Am. Phys. Soc. 20, 415 (1975).
[12]Y. Tomkiewicz, J. R. Andersen, and A. R. Taranko, Phys. Rev. B 17, 1579 (1978).
[13]K. Bechgaard, D. O. Cowan, and A. N. Bloch, J. Chem. Soc. Chem. Commun. 937 (1974).
[14]J. P. Ferraris, T. O. Poehler, A. N. Bloch, and D. O. Cowan, Tetrahedron Lett. 2553 (1973).
[15]J. Diekmann, W. R. Hertler, and R. E. Benson, J. Org. Chem. 28, 2719 (1963).
[16]L. B. Coleman, Rev. Sci. Instrum. 46, 1125 (1975).
[17]H. C. Montgomery, J. Appl. Phys. 42, 2971 (1971).
[18]P. M. Chaikin and J. F. Kwak, Rev. Sci. Instrum. 46, 218 (1975).
[19]R. P. Huebener, Phys. Rev. 135, A1281 (1964).
[20]H. E. Bennett, J. M. Bennett, and E. J. Ashley, J. Opt. Soc. Am. 52, 1245 (1962).
[21]J. R. Cooper, D. Jerome, M. Weger, and S. Etemad, J. Phys. Lett. (Paris) 36, L219 (1975).
[22]K. Bechgaard, C. S. Jacobsen, and N. Hessel Andersen, Solid State Commun. 25, 875 (1978).
[23]E. M. Engler, R. A. Craven, Y. Tomkiewicz, B. A. Scott, K. Bechgaard, and J. R. Andersen, J. Chem. Soc. Chem. Commun. 337 (1976).
[24]C. S. Jacobsen, J. R. Andersen, K. Bechgaard, and C. Berg, Solid State Commun. 19, 1209 (1976).
[25]A. A. Bright, A. F. Garito, and A. J. Heeger, Solid State Commun. 13, 943 (1973).
[26]J. B. Torrance, B. A. Scott, and F. B. Kaufman, Solid State Commun. 17, 1369 (1975).
[27]P. M. Grant, R. L. Greene, G. C. Wrighton, and G. Castro, Phys. Rev. Lett. 31, 1311 (1973).
[28]D. B. Tanner, C. S. Jacobsen, A. F. Garito, and A. J. Heeger, Phys. Rev. B 13, 3381 (1976).
[29]A. J. Berlinsky and J. F. Carolan, Solid State Commun. 15, 795 (1974).

[30]L. P. Gorkov and I. E. Dzyaloshinskii, Pis'ma Zh. Eksp. Teor. Fiz. 18, 686 (1975) [JETP Lett. 18, 401 (1973)].
[31]E. M. Conwell, Phys. Rev. Lett. 39, 777 (1977).
[32]F. Denoyer, R. Comes, A. F. Garito, and A. J. Heeger, Phys. Rev. Lett. 35, 445 (1975).
[33]C. Weyl, E. M. Engler, K. Bechgaard, G. Jehanno, and S. Etemad, Solid State Commun. 19, 925 (1976).
[34]R. Comes, Ann. N. Y. Acad. Sci. (to be published).
[35]T. Wei, S. Etemad, A. F. Garito, and A. J. Heeger, Phys. Lett. A 45, 269 (1973).
[36]P. M. Chaikin and G. Beni, Phys. Rev. B 13, 647 (1976).
[37]P. M. Chaikin, J. F. Kwak, T. E. Jones, A. F. Garito, and A. J. Heeger, Phys. Rev. Lett. 31, 601 (1973).
[38]P. M. Chaikin, R. L. Greene, S. Etemad, and E. Engler, Phys. Rev. B 13, 1627 (1976).
[39]T. E. Phillips, T. J. Kistenmacher, A. N. Bloch, J. P. Ferraris, and D. O. Cowan, Acta Crystallogr. B 33, 422 (1977).
[40]C. S. Jacobsen, K. Bechgaard, and J. R. Andersen, Lect. Notes Phys. 65, 349 (1977).
[41]C. S. Jacobsen (unpublished).
[42]A. A. Bright, A. F. Garito, and A. J. Heeger, Phys. Rev. B 10, 1328 (1974).
[43]See, for example, F. Wooten, *Optical Properties of Solids* (Academic, New York, 1972), p. 195 ff.
[44]A good discussion of why the bands have opposite shape is given by F. Herman, D. R. Salahub, and R. P. Messmer, Phys. Rev. B 16, 2453 (1977).
[45]J. J. Ritsko, D. J. Sandman, A. J. Epstein, P. C. Gibbons, S. E. Schnatterly, and J. Fields, Phys. Rev. Lett. 34, 1330 (1975).
[46]See, for example, M. J. Rice and N. O. Lipari, Phys. Rev. Lett. 38, 437 (1977), and references therein.
[47]C. K. Chiang, Marshall J. Cohen, P. R. Newman, and A. J. Heeger, Phys. Rev. B 16, 5163 (1977).
[48]L. B. Coleman, Ph.D. thesis (University of Pennsylvania, 1975) (unpublished); J. P. Ferraris and T. F. Finnegan, Solid State Commun. 18, 1169 (1976).
[49]J. Bardeen, Solid State Commun. 13, 357 (1973).
[50]H. Fröhlich, Proc. R. Soc. Lond. A 223, 296 (1954).
[51]J. F. Kwak, P. M. Chaikin, A. A. Russel, A. F. Garito, and A. J. Heeger, Solid State Commun. 16, 729 (1975).
[52]J. R. Cooper and D. Jerome (unpublished).
[53]D. Jerome, J. Phys. Lett. (Paris) 38, L489 (1977).
[54]A. Madhukar and M. H. Cohen, Phys. Rev. Lett. 38, 85 (1977).
[55]S. Etemad, T. Penney, E. M. Engler, B. A. Scott, and P. E. Seiden, Phys. Rev. Lett. 34, 741 (1975).
[56]H. Gutfreund and M. Weger, Phys. Rev. B 16, 1753 (1977).
[57]T. J. Kistenmacher, T. E. Phillips, and D. O. Cowan, Acta Crystallogr. B 30, 763 (1974).
[58]For a review, see, J. Appel, in *Solid State Physics*, edited by F. Seitz, D. Turnbull, and H. Ehrenreich (Academic, New York, 1968), Vol. 21.
[59]P. M. Chaikin, A. F. Garito, and A. J. Heeger, Phys. Rev. B 5, 4966 (1972); J. Chem. Phys. 58, 2336 (1973).
[60]B. Horovitz, H. Gutfreund, and M. Weger, Phys. Rev. B 12, 3174 (1975).
[61]J. M. Ziman, *Electrons and Phonons* (Oxford University, London, 1960), p. 426.
[62]S. Etemad, Phys. Rev. B 13, 2254 (1976).